

The Effects of Ultraviolet Radiation on Nucleoside Modifications in RNA

Congliang Sun, Manasses Jora, Beulah Solivio, Patrick A Limbach* and Balasubrahmanyam Addepalli*

Rieveschl Laboratories for Mass Spectrometry, Department of Chemistry, University of Cincinnati, Cincinnati, Ohio 45221-0172, United States

Supplemental information

Experimental section

Nucleoside analysis by HR-LC-MS

The UVA-exposed and unexposed tRNAs were hydrolyzed to ribonucleosides as described before.¹ The RNA hydrolysates were subjected to high resolution liquid chromatography coupled with mass spectrometry (HR-LC-MS) using a Vanquish UHPLC system coupled to an Orbitrap Fusion LumosTM (Thermo Scientific) mass spectrometer. The hydrolyzed nucleosides were reconstituted in mobile phase A (5 mM ammonium acetate pH 5.3, MPA) and resolved on a HSS T3 column (100 Å, 1.8 µm, 2.1 x 50 mm, Waters) using a gradient of Mobile Phase B (60% H₂O, 40% acetonitrile, MPB) at 30 °C. After the elution of nucleosides under isocratic conditions (99 %A and 1 %B) for 6.3 min, MPB was progressively increased from 1-2% in 9.2 min., 3% in 16 min., 5% in 21.4 min., 25% in 24.6 min., 50% in 26.9 min. 75% in 30.2 min (hold of 0.3 min), 99% in 35 min (hold of 0.8 min) before reverting to isocratic conditions (99 %A, 1 %B) at 250 µL/min. Mass spectra were recorded in positive polarity under optimal electrospray conditions (capillary temperature 329 °C, spray voltage 3.5 kV, and 38, 11, 1 arbitrary units of sheath, auxiliary and sweep gas, respectively). The full-scan mass spectra were acquired in the Orbitrap mode (m/z 105-900) at 120,000 mass resolution at a mass accuracy of <4 ppm. Tandem mass spectrometry (MS/MS) by collision-induced dissociation (CID, 42% collision energy) was used in data-dependent mode to switch automatically between MS (scan 1), and four CID scans to record the fragmentation products of nucleosides. The identification criteria of modified nucleosides include relative retention time, high resolution molecular mass and MS/MS behavior. The accurate m/z values of the conversion products were computed by ChemCalc (http://www.chemcalc.org/mf_finder/mfFinder_em_new). The peak areas of individual

nucleosides were computed using the Quan browser of Xcalibur. Differences in the levels of damaged nucleosides and other modifications are normalized against the peak area of its corresponding canonical nucleoside as described before² and computing the percent change, or by computing the fold-change between UVA-exposed and unexposed control.

Supplemental Figure legends

Supplemental Figure S1. Effect of riboflavin concentration and UVA exposure time on oxidation of purines in tRNA. Oxidation pathway of guanosine (scheme 1)³ and adenosine (scheme 2)⁴ are shown.

- A. Effect of riboflavin: Five micrograms of *E. coli* tRNA was exposed to UVA for 20 min at 0, 10, 100 and 1000 μ M riboflavin, and analyzed for oxidized purines by LC-MS. (i) Comparative levels of 8-oxoguanosine (8-oxo-rG) and 5-guanidinohydantoin ribonucleoside (Gh) as a fraction of the observed guanosine is shown. (ii) Comparative levels of 8-oxoadenosine (8-oxo-rA) and 4,6-diamino-5-formamidopyrimidine (FapyA) as a fraction of the observed adenosine signal is shown.
- B. Effect of UVA exposure time: Five micrograms of *E. coli* tRNA was exposed to UVA for 0-30 min in the presence of 100 μ M riboflavin, and analyzed for oxidized purines by LC-MS. (i) Comparative levels of 8-oxo-rG and Gh as a fraction of the observed guanosine is shown. (ii) Comparative levels of 8-oxo-rA and FapyA as a fraction of the observed adenosine signal is shown.

Supplemental Figure S2: LC-MS analysis of ¹⁵N-labeled tRNA for oxidized guanosine and adenosine photoproducts following exposure to UVA. Five micrograms of ¹⁵N-labeled tRNA was exposed to UVA in presence of 100 μ M riboflavin for 20 min. Incorporation of ¹⁵N leads to mass shift of purine ribonucleoside by +4.9852 Da.

- (A) LC-MS analysis of ¹⁵N-labeled Gh in the UVA exposed tRNA compared to unexposed sample. (i) Extracted ion chromatogram (XIC) for m/z 295.0952 corresponding to Gh in the 'No UVA' (top panel) and UVA (bottom panel) are shown. (ii) Mass spectrum (top panel) of the XIC of UVA exposed sample depicts the presence of ribonucleoside-Gh molecular ion (m/z 295.0943, error 3 ppm). Its tandem mass spectrum (bottom panel) indicates the presence of nucleobase ion (loss of ribose sugar-132 Da).
- (B) LC-MS analysis of ¹⁵N-labeled FapyA in the UVA exposed tRNA compared to unexposed sample. (i) XIC for m/z 291.1003 corresponding to FapyA in the 'No UVA' (top panel) and UVA (bottom panel) are shown. (ii) Mass spectrum (top panel) of the XIC of UVA exposed sample depicts the presence of ribonucleoside - FapyA molecular ion (m/z 291.0994, error 3 ppm). Its tandem mass spectrum (bottom panel) shows the presence of nucleobase ion (m/z 159) and a number of fragment ions including loss of water.

Supplemental Figure S3: LC-MS analysis of UVA or riboflavin (RF)-induced effect on tRNA modifications, s^2C and ms^2i^6A .

(A) Effect of UVA alone on s^2C . (i) Extracted ion chromatogram (XIC) for m/z 260.0706 corresponding to s^2C in the 'No UVA' (top panel) and UVA alone (bottom panel) are shown. (ii) Mass spectrum (top panel) of 'no UVA' XIC depicts the presence of s^2C molecular ion (m/z 260.0701, error 2 ppm), and tandem mass spectrum (bottom panel) shows the unique fragmentation of s^2C .

(B) Effect of RF alone on ms^2i^6A . (i) Extracted ion chromatogram (XIC) for m/z 382.1549 corresponding to ms^2i^6A in the 'No UVA' (top panel) and RF alone (bottom panel) are shown. (ii) Mass spectrum (top panel) of 'no UVA' XIC depicts the presence of ms^2i^6A molecular ion (m/z 382.1545, error 1 ppm), and tandem mass spectrum (bottom panel) shows the presence of nucleobase ion.

Supplemental Figure S4: LC-MS based detection of UVA-induced photoproduct, mnm^5U following exposure of *E. coli* tRNA to UVA.

(A) LC-MS analysis of mnm^5U formed following UVA exposure compared to unexposed sample. (i) XIC for m/z 288.1196 corresponding to mnm^5U in the 'No UVA' (top panel) and UVA (bottom panel) are shown. (ii) Mass spectrum (top panel) of the XIC of UVA exposed sample depicts the presence of molecular ion (m/z 288.1192, error 1 ppm). Its tandem mass spectrum (bottom panel) shows the presence of nucleobase ion (m/z 156).

(B) LC-MS analysis of ^{15}N -labeled mnm^5U formed following UVA exposure compared to unexposed sample. (i) XIC for m/z 291.1107 corresponding to ^{15}N -labeled mnm^5U in the 'No UVA' (top panel) and UVA (bottom panel) are shown. (ii) Mass spectrum (top panel) of the XIC of UVA exposed sample depicts the presence of molecular ion (m/z 291.1098, error 3 ppm). Its tandem mass spectrum (bottom panel) shows the presence of nucleobase ion (m/z 159).

Supplemental Figure S5: LC-MS analysis of the emergence of UV-induced photoproduct, nm^5U , following exposure of *E. coli* tRNA to UVA for 20 min.

(A) LC-MS analysis of the emergence of nm^5U in the UVA exposed tRNA compared to unexposed sample. (i) XIC for m/z 274.1039 corresponding to nm^5U in the 'No UVA' (top panel) and UVA (bottom panel) are shown. (ii) Mass spectrum (top panel) of XIC illustrating the nm^5U molecular ion (m/z 274.1035, error 1 ppm), and its tandem mass spectrum (bottom panel) illustrates the appearance of nucleobase ion (m/z 142).

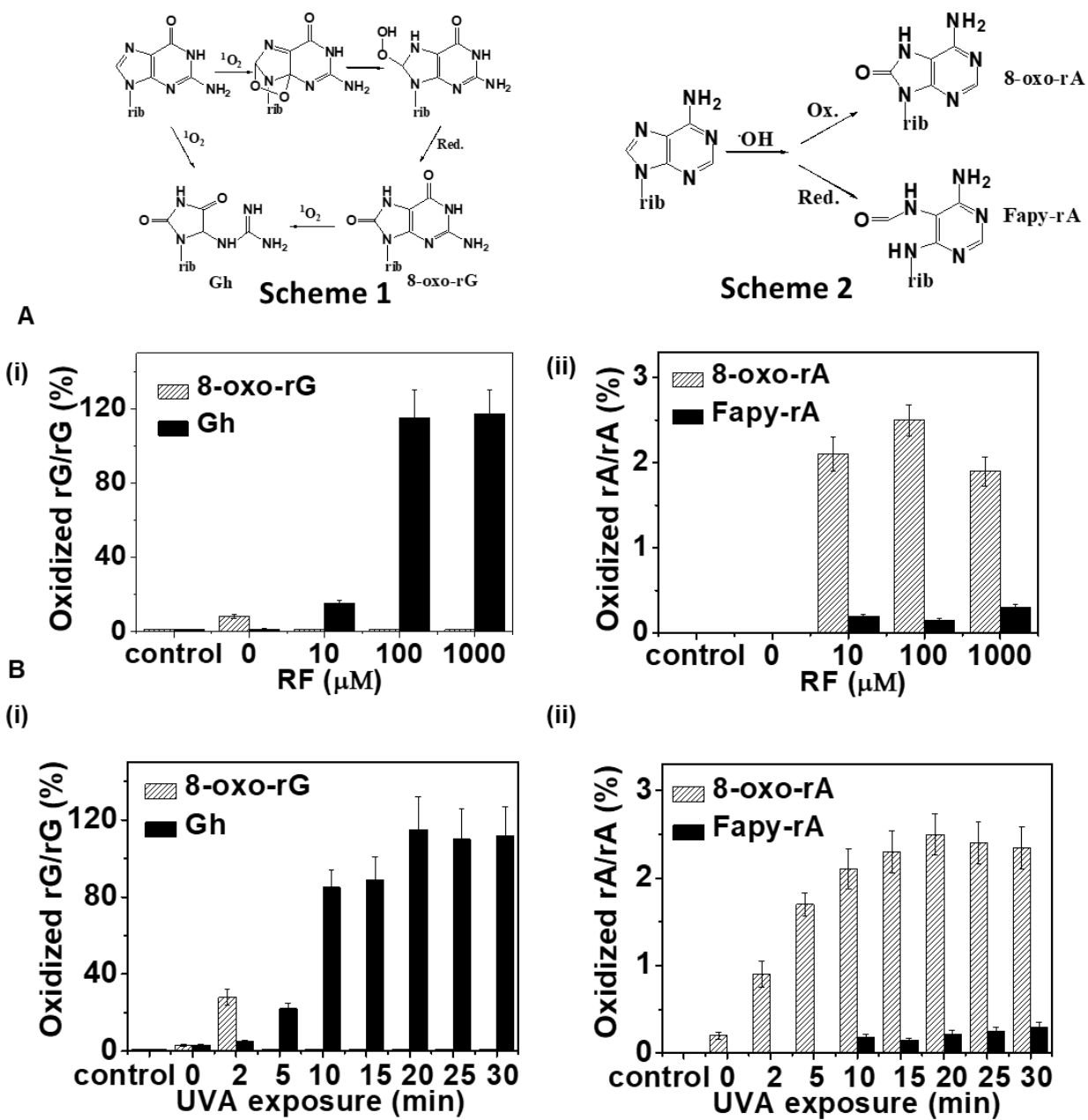
(B) LC-MS analysis of the emergence of ^{15}N -labeled nm^5U in the UVA exposed ^{15}N -labeled tRNA compared to unexposed sample. (i) XIC for m/z 277.0950 corresponding to ^{15}N -labeled nm^5U in the 'No UVA' (top panel) and UVA (bottom panel) are shown. (ii) Mass spectrum (top panel) of XIC depicting ^{15}N -labeled nm^5U molecular ion (m/z 277.0960, error 4 ppm), and its tandem mass spectrum (bottom panel) shows the presence of nucleobase ion (m/z 145).

Supplemental Figure S6: LC-MS based detection of 5-methoxyuridine (mo⁵U) and 5-hydroxyuridine (ho⁵U) following UVA exposure of cmo⁵U. Two micrograms of cmo⁵U was exposed to UVA in presence of 100 μ M riboflavin for 20 min.

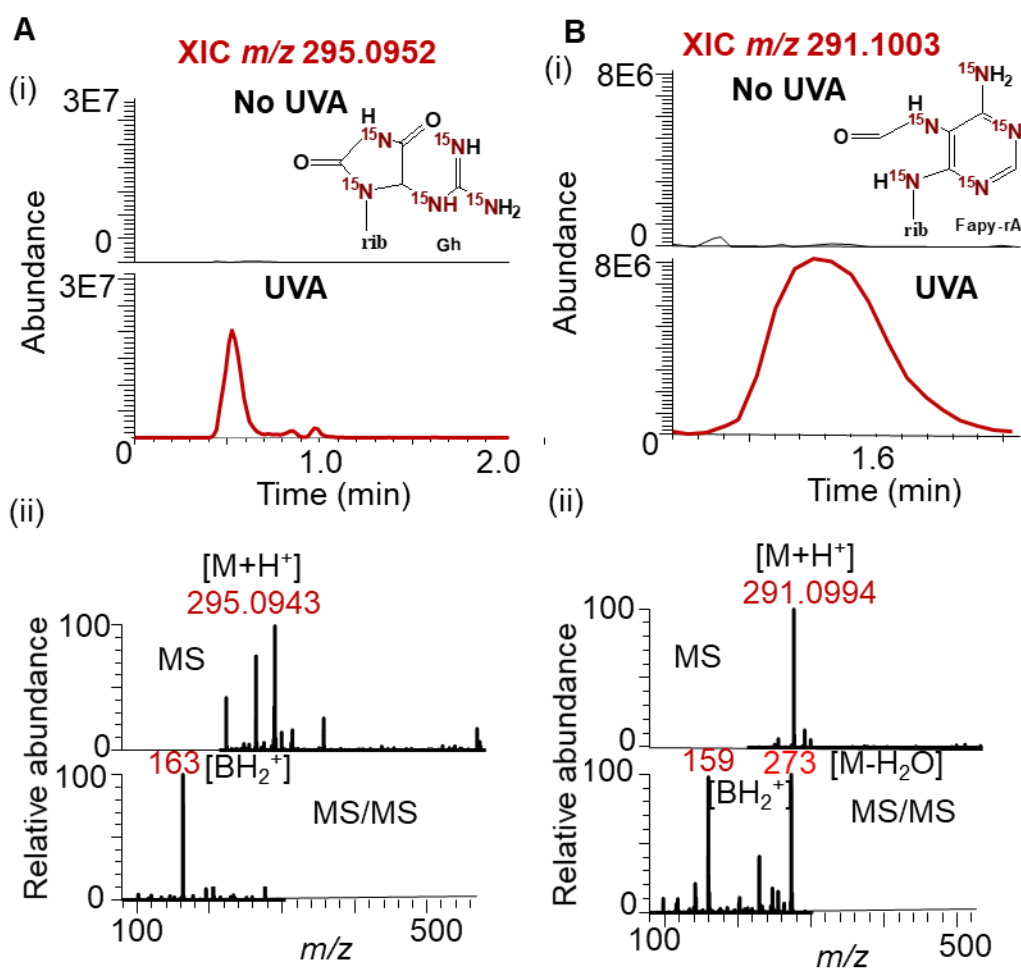
- (A) Detection of mo⁵U. (i) XIC for m/z 275.0879 corresponding to mo⁵U in the ‘No UVA’ (top panel) and UVA (bottom panel) are shown. (ii) Mass spectrum (top panel) of ‘UVA’ XIC depicts the presence of molecular ion (m/z 275.0871, error 3 ppm), and its tandem mass spectrum (bottom panel) shows the presence of nucleobase ion (m/z 143).
- (B) Detection of ho⁵U. (i) XIC for m/z 261.0723 corresponding to ho⁵U in the ‘No UVA’ (top panel) and UVA (bottom panel) are shown. (ii) Mass spectrum (top panel) of ‘UVA’ XIC depicts the presence of molecular ion (m/z 261.0715, error 3 ppm), and its tandem mass spectrum (bottom panel) shows the presence of nucleobase ion (m/z 129).

Supplemental Figure S7: Increased susceptibility of *E. coli* mutant $\Delta trmU$ to UVA (3 mJ cm⁻²).

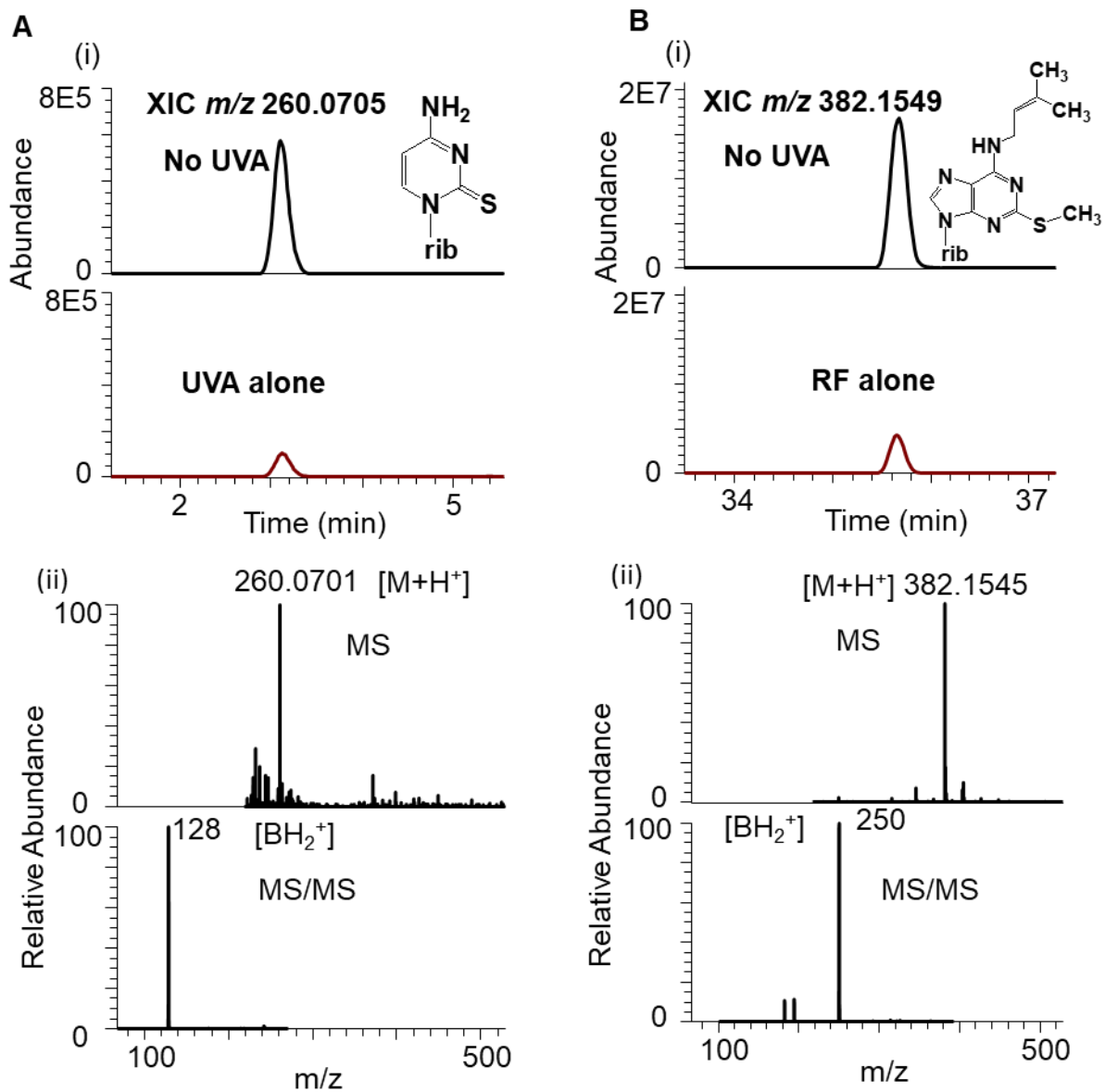
Percent survival of UVA exposed cells compared to unexposed cells is plotted for wild-type K-12 MG1655 (blue line), and mutant $\Delta trmU$ (red line). Data represent mean \pm SD values of four biological replicates.



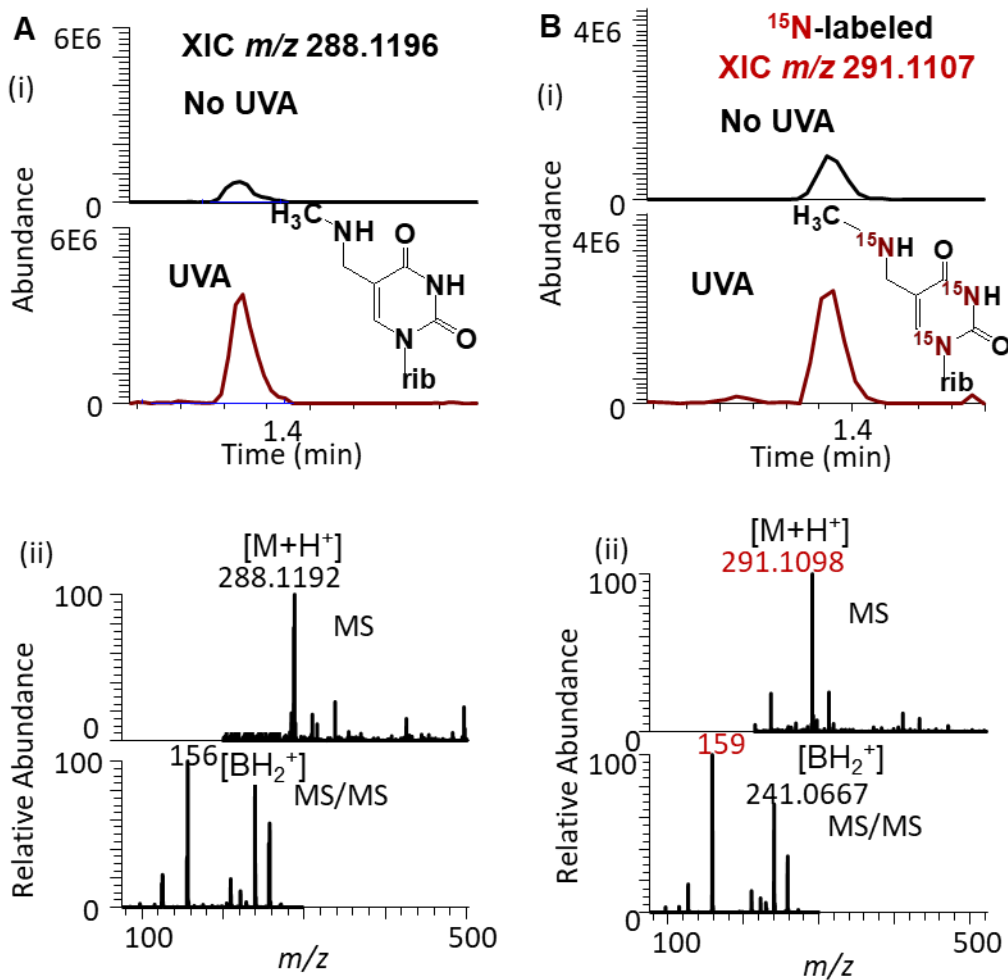
Supplemental Figure S1



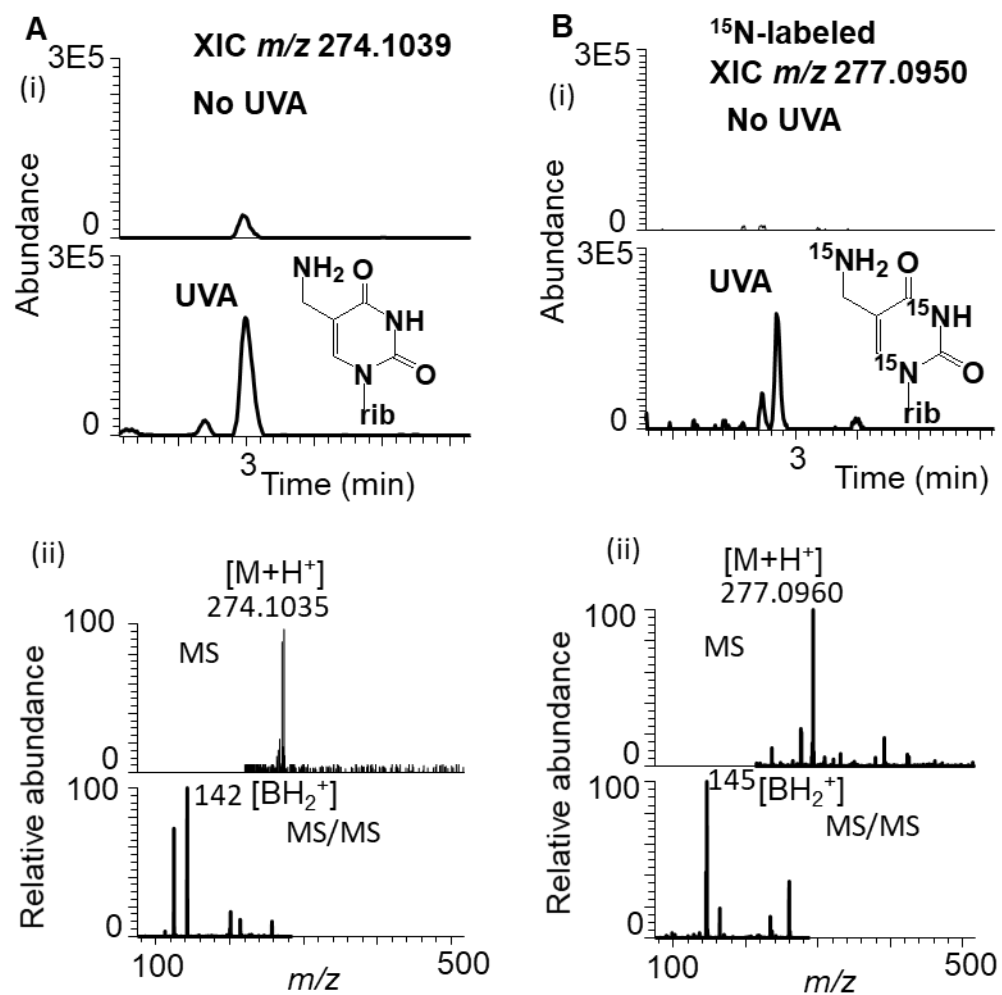
Supplemental Figure S2



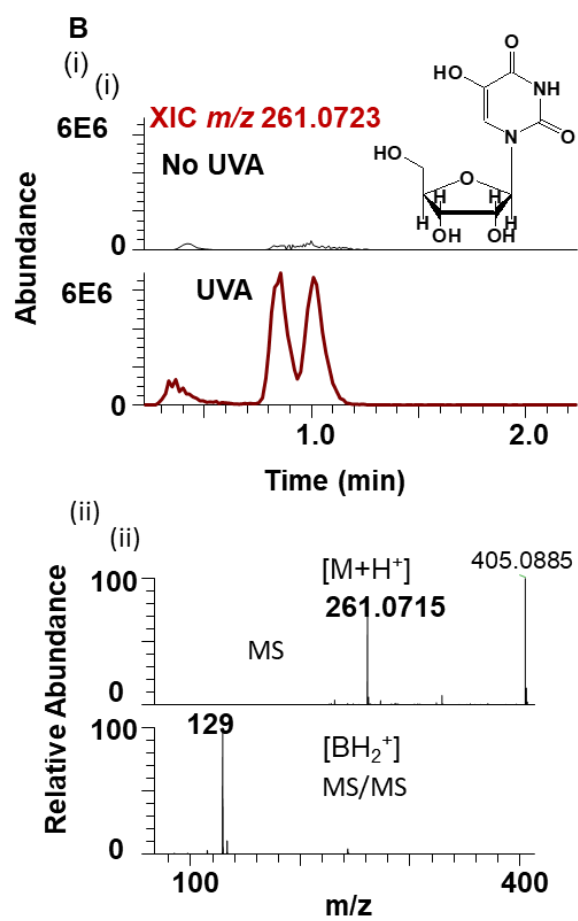
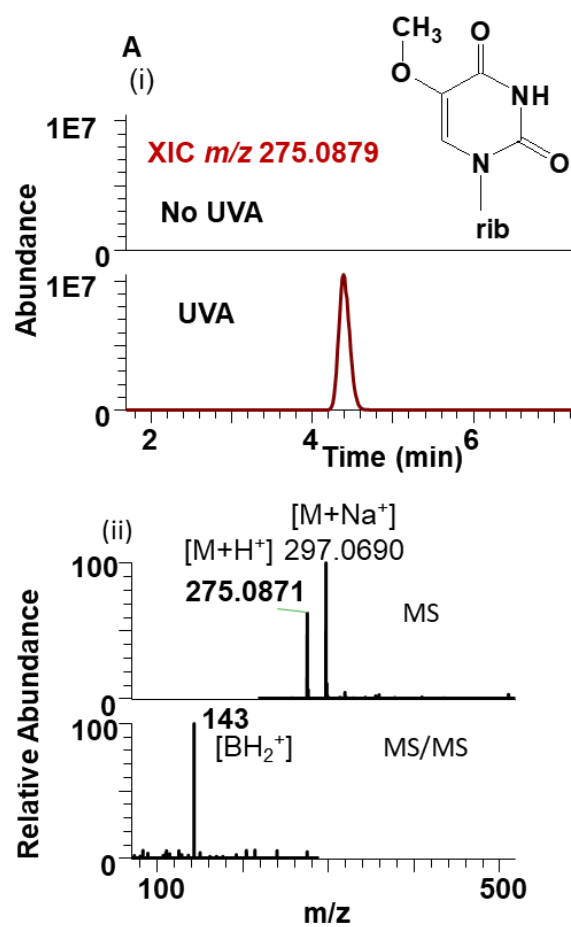
Supplemental Figure S3



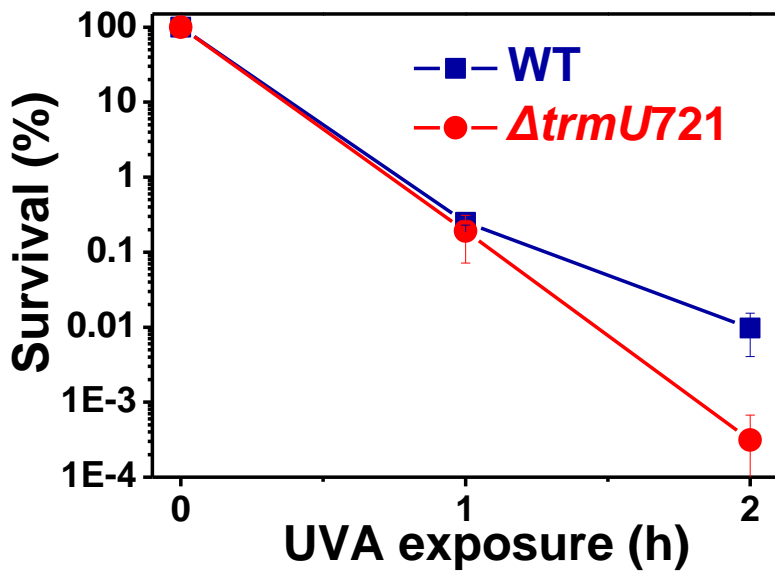
Supplemental Figure S4



Supplemental Figure S5



Supplemental Figure S6



Supplemental Figure S7

References

- [1] Russell, S. P., and Limbach, P. A. (2013) Evaluating the reproducibility of quantifying modified nucleosides from ribonucleic acids by LC-UV-MS, *J. Chromatogr. B: Anal. Technol. Biomed. Life Sci.* 923-924, 74-82.
- [2] Jia, G., Fu, Y., Zhao, X., Dai, Q., Zheng, G., Yang, Y., Yi, C., Lindahl, T., Pan, T., Yang, Y. G., and He, C. (2011) N6-methyladenosine in nuclear RNA is a major substrate of the obesity-associated FTO, *Nat. Chem. Biol.* 7, 885-887.
- [3] Ravanat, J. L., Douki, T., and Cadet, J. (2001) Direct and indirect effects of UV radiation on DNA and its components, *J. Photochem. Photobiol., B* 63, 88-102.
- [4] Cadet, J., Douki, T., Ravanat, J. L., and Di Mascio, P. (2009) Sensitized formation of oxidatively generated damage to cellular DNA by UVA radiation, *Photochem. Photobiol. Sci.* 8, 903-911.